



Removal of Amoxicillin in Wastewater Using Advanced oxidation process by $ZnFe_2O_4$ and $CoFe_2O_4$ and Oxidation with Hydrogen Peroxide

VanamSudhakar^{1*} | S.Srinu Naik² | T.Nagaveni³ | T.Shwetha Shree⁴

^{1*}Research Scholar, ²Professor, Department of Chemical Engineering, University College of Technology, Osmania University, Hyderabad, Telangana, INDIA

³Associate Professor, Department of Mechanical Engineering, University College of Engineering, Osmania University, Hyderabad, Telangana, INDIA

⁴M.tech Student, Department of Chemical Engineering, University College of Technology, Osmania University, Hyderabad, Telangana, INDIA

Email id: suddhu.vanam@gmail.com

To Cite this Article

Vanam Sudhakar, S.Srinu Naik, T.Nagaveni and T.Shwetha Shree Removal of Amoxicillin in Wastewater Using Advanced oxidation process by $ZnFe_2O_4$ and $CoFe_2O_4$ and Oxidation with Hydrogen Peroxide. *International Journal for Modern Trends in Science and Technology* 2022, 7 pp. 452-458. <https://doi.org/10.46501/IJMTST0712082>

Article Info

Received: 29 November 2021; Accepted: 28 December 2021; Published: 03 January 2022

ABSTRACT

Antibiotics disposed into wastewater reach wastewater treatment plants and surface waters and act as micro-pollutants. As antibiotics pose various problems related to treatment and reuse, it is imperative to remove them from wastewater. In the present paper, adsorption studies have been carried out for removal of amoxicillin using Zinc ferrite ($ZnFe_2O_4$) in a batch mode and Zinc ferrite ($CoFe_2O_4$). Removal of antibiotics has also been made using oxidation by H_2O_2 . The techniques used for detection of antibiotics require elaborate analytical instrumentation. Being inexpensive and simple technique, monitoring of concentration during removal has been made using COD determination in the present work. The XRD peaks, structural analysis of $ZnFe_2O_4$ and $CoFe_2O_4$ nanosamples, were Zinc ferrite the average particle size obtained varied between 18.63-20.45 nm. Similarly, for Cobalt ferrite, the average particle size obtained varied between 18.54-18.90 nm based on the 2θ values. In FTIR Zinc Nano-ferrite exhibits two absorption bands in this region. High vibration band at 557.22 cm^{-1} and others were at 446.5 cm^{-1} . Zinc ferrite is exhibiting an inverse spinel where Fe^{3+} ions and Zn^{2+} ions present at the tetrahedral and octahedral lattice. Cobalt nano-ferrite exhibits two absorption bands in this region. High vibration band at 570.41 cm^{-1} and others were at 443.24 cm^{-1} . $CoFe_2O_4$ is exhibiting an inverse spinel where Fe^{3+} ions and Co^{2+} ions present at the tetrahedral and octahedral lattice sites respectively. SEM Image of Nano Zinc ferrite and Cobalt ferrites show the size of the particle is around 340 nm., Cobalt ferrites size was found to be 308.8 nm. The degradation of AMX is 78.04%, with $ZnFe_2O_4$ in Fenton oxidation. The degradation of AMX is 84.01%, with $CoFe_2O_4$ in Fenton oxidation. However, during the Photo-Fenton oxidation, The degradation of AMX is 95.89% with $ZnFe_2O_4$ and The degradation of AMX is 97.54%, with $CoFe_2O_4$ in photo-Fenton oxidation. Mineralization of AMX is 71.02%, with $ZnFe_2O_4$ in Fenton oxidation. The degradation of AMX is 79.15%, with $CoFe_2O_4$ in Fenton oxidation. Similarly during the Photo-Fenton oxidation, mineralization of AMX is 91.75% with $ZnFe_2O_4$ and The degradation of AMX is 93.52%, with $CoFe_2O_4$ in photo-Fenton oxidation. Therefore, Fenton and Photo-Fenton oxidation using cobalt ferrite catalyst appears to be an effective and economical for the oxidation of AMX, in aqueous solution.

Keywords: Advanced oxidation process, Amoxicillin, Hydrogen peroxide, Zinc ferrite and Cobalt ferrite

1. INTRODUCTION

Antibiotics are of great importance for therapeutic purposes in human and veterinary medicine [1]. The presence of antibiotics detected in aquatic environment becomes important as it leads to rise of refractory and even toxic pollutants. Presence of antibiotics in wastewater arises from different sources like discharge from domestic wastewater treatment plants (WWTP) [2], pharmaceutical companies [3], runoff from animal feeding operation, and from compost made of animal manure containing antibiotics [4], and by application of antibiotics on livestock production [5]. Excreted non-metabolized antibiotics enter wastewater streams through hospital effluent and domestic sewage systems [1]. If antibiotics are not degraded or eliminated during sewage treatment, they reach surface water, groundwater and drinking water [6]. In WWTP, the presence of antibiotics make an increase in organic load and may disturb the process of biological removal of organic matter. COD removal efficiency also decreases due to bacterial toxicity of antibiotics and their recalcitrance [7,8]. Moreover, the characteristics like toxicity, biodegradability and inhibition has a correlation with their removal in biological treatment [9]. The appearance of bacterial strains that are resistant to antibiotics is a result of abuse of antibiotics. This phenomenon is known as antibiotic resistance [10]. The presence of antibiotics in wastewater may cause bacterial resistance in human beings and livestock when water is reused. The selection and development of antibiotic-resistant bacteria is one of the greatest concerns with regard to the use of antimicrobials [6]. Enteric microorganisms carrying resistance genes are found in WWTP. Development of antibiotic resistance in pathogens causes problems in clinical treatment and serious problems for human health [11]. In industry, presence of antibiotics in water may inhibit bacterial culture during fermentation process. It is apparent that impurities in the waste fermentation broth, particularly biopolymers or macromolecules can seriously affect the crystallization of antibiotics. The residual antibiotics in the fermentation waste not only cause the loss of product but also suppress microbial growth in downstream biological wastewater treatment [12]. Hence, it is imperative to remove antibiotics from wastewater. There are several methods available for removal of antibiotics from wastewater. It includes

coagulation [13], adsorption [14], oxidation using chlorination [15], ozonation [16], H_2O_2 , UV light, biological anaerobic process through UASB [7], membrane separation, ultrafiltration, reverse osmosis [10,17], and electrochemical removal [18]. Extent of removal and rates vary greatly depending on the treatment utilized, its duration and the concentration and physical properties of the pharmaceuticals in the influent.

The aim of the present investigation is to study the paracetamol degradation and chemical oxygen demand (COD) removal efficiencies by Fenton and photo-Fenton processes. The oxidation experiments are carried out at ambient temperature ($27 \pm 3^\circ C$) in batch reactors. The purpose of this work is to remove amoxicillin as well as to evaluate percentage removal of amoxicillin using $ZnFe_2O_4$ and $CoFe_2O_4$ in continuous and batch modes respectively. The effect of initial paracetamol concentration on the degradation and mineralization of paracetamol by both Fenton oxidation and Photo-Fenton oxidation are evaluated and the results are compared. Paracetamol samples are analyzed using a UV-Vis spectrophotometer.

2. MATERIALS AND METHODS

2.1 Materials

Paracetamol extra pure (98% assay) is purchased from Bangalore fine chem (India). Hydrogen peroxide (H_2O_2) (50% w/w) and ferrous sulfate ($FeSO_4 \cdot 7H_2O$) are purchased from Molychem (India). The chemicals are used as received in the Fenton oxidation process. Hydrochloric acid (HCl, Molychem, India, 35% purity), sulfuric acid (H_2SO_4 , SD Fine Chem. Ltd, India, 98% purity), sodium hydroxide (NaOH, Molychem, India, 98% purity), are also used in the experiments. Methanol AR grade (Merck, India), The simulated paracetamol aqueous stock solution of 1,000 mg/L concentration is prepared every week with deionized water and stored in the dark at $4^\circ C$.

2.2 Synthesis of $ZnFe_2O_4$ and $CoFe_2O_4$ Nanoparticles

Zinc ferrite nanoparticles were synthesized by co-precipitation method, using starting material of iron nitrate nonahydrate ($Fe(NO_3)_3 \cdot 9H_2O$) and Zinc nitrate hexahydrate ($Zn(NO_3)_2 \cdot 6H_2O$). 30 ml of 0.2 M zinc nitrate solution were mixed with 30 ml of 0.4 M iron nitrate solution in 500 ml beaker. The initial pH of the solution was noted as 1.14 because of the presence of

nitric and nitrous acids. The solution was constantly stirred with the help of magnetic stirrer. 10-15 ml of 3 M solution of NaOH was added drop wise to adjust the pH of solution 11-12, with constant stirring. The reaction is carried out in higher values of pH, because in this pH range the size of the particles as well as their nucleation rate is controlled [19]. A little amount of oleic acid 4-5 drops were added to the solution. Oleic acid prevents the agglomeration of the nanoparticles. The solution was then brought to reaction temperature of 80°C. The solution was stirred for 60 minutes and subsequently cooled to room temperature. The solution was decanted and washed twice with distilled water and finally with ethanol to remove the impurities and excess surfactant. The as-synthesized nanoparticles were centrifuged for 15 minutes at 3500 rpm and dried overnight at 105°C. The dried particles were milled in agate mortar. The powder nanoparticles were annealed at temperature of 400 °C, for 4 hours.

Cobalt ferrite catalyst was synthesized by using one molar $\text{Fe}(\text{NO}_3)_3 \cdot 9\text{H}_2\text{O}$ and one molar $\text{Co}(\text{NO}_3)_2 \cdot 6\text{H}_2\text{O}$ in double distilled water. These solutions were mixed in 1:2 ratio with constant stirring at 70°C for one hour. 25% ammonia solution was used for precipitation and controlling pH of solution 10.5. The precipitated material was washed with hot double distilled water and ethanol number of times to remove unwanted residual left over salts. The precipitates were filtered and then dried at 105°C to obtain fine powder. The dried fine powder was annealed at 350°C in muffle furnace.

2.3 characterization of catalysts

Powder X-Ray diffraction analysis (XRD) was carried out for the calcined samples with a Bruker D8 model analytical Instrument Facility at Hyderabad central university (HCU), Hyderabad. The XRD patterns were recorded on the X-ray diffractometer at the range of 2θ from 10° to 90°, using Cu target X-Ray tube, $\text{Cu K}\alpha$ ($\lambda = 1.5406 \text{ \AA}$) radiation with an accelerating voltage of 40 kV. FT-IR study was accomplished in order to confirm the formation of nano particle in the range of 4500-400 cm^{-1} by instrumentation using the model Shimadzu-8400S analytical Instrument Facility at Hyderabad central university (HCU), Hyderabad. The particles size and morphology of the synthesized sample has been studied by The SEM analysis is carried

out with the help of computer controlled field emission scanning electron microscope HITACHI S-3700N. The working conditions are set at an accelerating voltage of 0.5 kV to 30kV, resolution: 4 nm (30kV), magnification: 300,000.

2.3.1 X-ray diffraction analysis (XRD)

The XRD peaks, structural analysis of ZnFe_2O_4 and CoFe_2O_4 nanosamples, were studied with Sherrer's equation, zinc ferrite the average particle size obtained varied between 18.63-20.45 nm based on the 2θ value, which was found to be 30.30, 35.45, 43.05, and 56.85, respectively. Cubic phase structure of the zinc ferrite rendered by the JCPDS 22-1012 card.

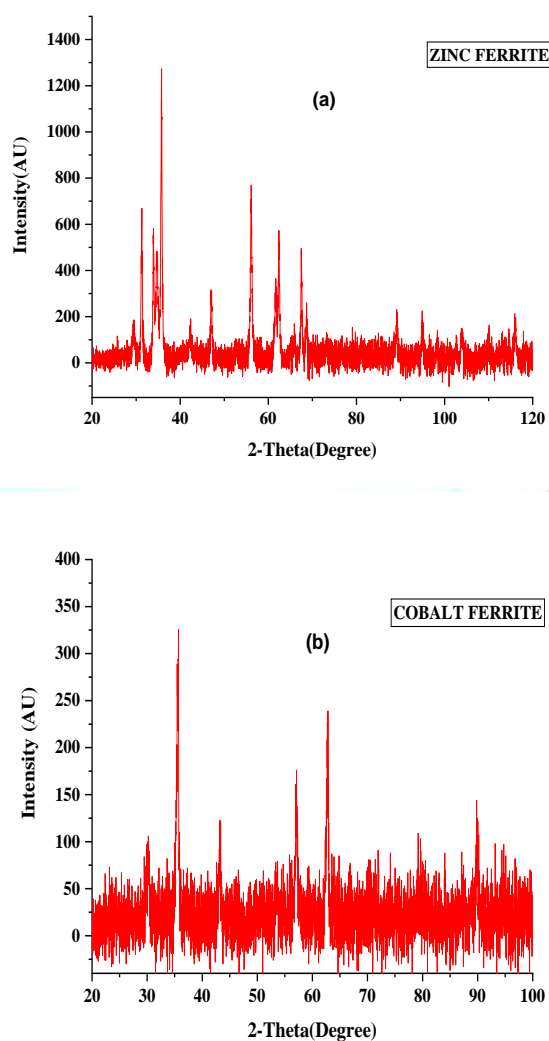


Figure.1(a)&(b):XRD peaksof spinelnano ferrites

Similarly, for Cobalt ferrite, the average particle size obtained varied between 18.54-18.90 nm based on the 2θ

value which was found to be 35.64, 40.58.70 and 62.60 respectively. Sample possessed a cubic spinel structure. Size and shapes define the XRD peak position and intensity defines the atomic position of the unit cell. Table.1.XRDValuesofMetal NanoFerrite

Nano Zinc Ferrite		
2θ	λ	Particlesize (nm)
30.1008	400	18.63
35.4579	654	18.89
56.7441	340	20.45
Nano Cobalt Ferrite		
2θ	λ	Particlesize (nm)
27.6962	545	18.54
33.2055	595	18.78

Fourier-Transform-InfraredSpectroscopy(FTIR)

An important tool, Infrared spectroscopy which made an investigation of the spinel structural formation of ferrite nanoparticles. This provides information about positions of the metal cation in the spinel structure and their vibrational modes. In the case of ferrites, the oxygen ions vibrate with cations of the unit cell in the octahedral and tetrahedral sites are responsible for absorptions bands. For spinel ferrites, a specific region of absorption is in the range of 400–600 cm⁻¹. Figure.2 (A) shows Zinc Nano-ferrite exhibits two absorption bands in this region. High vibration band at 557.22 cm⁻¹ and others were at 446.5 cm⁻¹. Zinc ferrite is exhibiting an inverse spinel where Fe³⁺ ions and Zn²⁺ ions present at the tetrahedral and octahedral lattice.

Figure.2(B) shows Cobalt nano-ferrite exhibits two absorption bands in this region. High vibration band at 570.41 cm⁻¹ and others were at 443.24 cm⁻¹. Absorption bands detected within this region disclose the creation of single-phase spinel structure having two sub-lattices, octahedral and tetrahedral. CoFe₂O₄ is exhibiting an inverse spinel where Fe³⁺ ions and Co²⁺ ions present at the tetrahedral and octahedral lattice sites respectively. The vibration observed due to bending was very broad.

The reason could be attributed to the distribution of Fe³⁺ ions leading to vibrations due to the stretching mode of the (Fe³⁺)–oxygen bond at tetrahedral, and other caused due to (Co²⁺)–oxygen vibrations in octahedral sites.

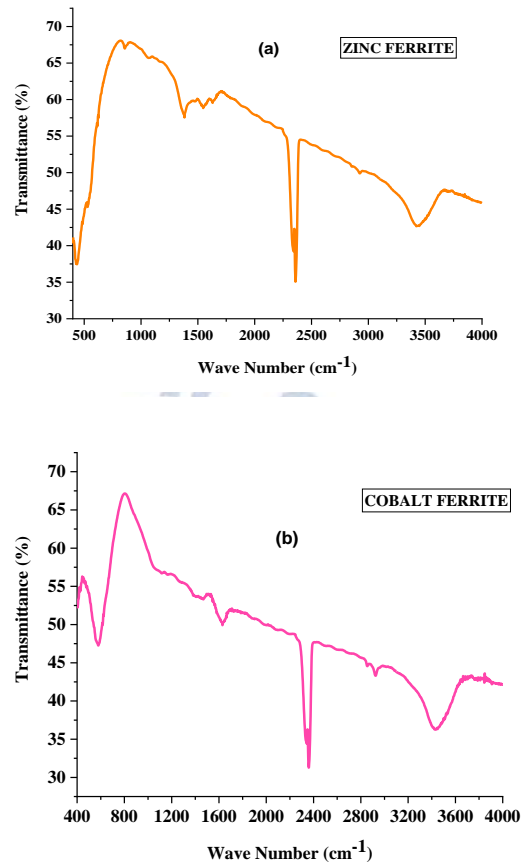


Figure.2(a)&(b):FTIRbands of spinel nanoferrites

2.3.3 Scanning Electron Microscopy (SEM)

Images of SEM reveal surface topography and composition of the sample. The surface morphological images and Microscopic structure shows a good agreement with XRD results of ferrite nanoparticles. Images suggest that morphology at the surface is porous in nature, it is happening because of the significant degree of agglomeration of ferrite particles.

SEM Image Nano Zinc ferrites show the size of the particle is around 340 nm. From the images shown in image Figure 3(a), we can infer that the particles are of irregular shape and agglomerated together. There was a significant trace of carbon seen. The agglomeration of the particles may be due to the hydrophilic nature of the extract added. The traces of carbon observed may be due to the usage of the mica sheet as a substrate for the sample.

SEM Image Nano Cobalt ferrites show a zoomed view of the powdered sample, illustrated with both large and small grains. Then an particle size was found to be 308.8 nm. From

the images shown in Figure 3 (b), we can infer that the particles are of irregular shape and are agglomerated together to form a bigger Particle. There was a considerable trace of carbon seen. The agglomeration of the particles may be due to the hydrophilic nature of the extract added. The traces of

carbon observed may be due to the usage of the mica sheet as a substrate for this sample.

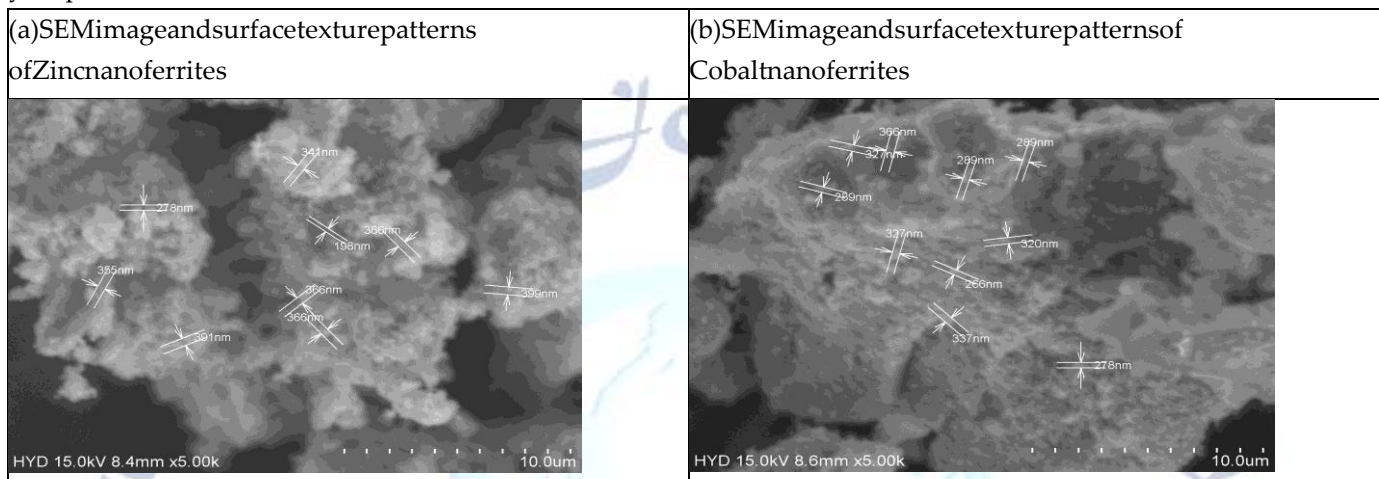


Figure.3(a)&(b): SEM images of spinel nano ferrites

3. EXPERIMENTAL PROCEDURE

Fenton oxidation: Batch experiment was conducted for the degradation study with continuous stirring. A 1000 ml capacity cylindrical borosilicate vessel was used as the reactor. 0.1N H₂SO₄ and 0.1N NaOH used for the adjustment of drug solution pH prior to addition of catalyst. Ferrite was added and mixed for about 10 min at 250 rpm using magnetic stirrer and solution pH was recorded. The initial concentration of AMX, PCM and KTP were of 20 to 80 mg/L, respectively. pH was varied from 2.0 to 10.0, 2.0 to 4.0 and 2.0 to 5.0 for AMX, PCM and KTP, respectively. Catalyst doses were of 0.25 to 1.25 mg/L. The subsequent H₂O₂ was in the range of mg/L. 10 mL sample was taken out at different time intervals and 0.1 N NaOH was immediately added to stop the reaction at 10:1 (v/v). NaOH addition increased pH around from 12.0. Sludge was separated out by centrifugation at 2000 rpm for 30 min and clear supernatant was heated at 70°C to destroy residual H₂O₂. The aliquot of drug solutions are taken out for analysis at pre-defined time intervals and filtered through 0.45 μm Millipore filter for COD analysis and for determination of AMX, PCM and KTP concentrations by using UV-VIS Spectrophotometer.

Photo-Fenton oxidation: The photocatalytic activities of the synthesized ZnFe₂O₄ and CoFe₂O₄ samples were quantified by measuring the rates of Photo-Fenton oxidation of different Pharmaceutical compounds. The experiments were performed in indigenously prepared immersion type Photocatalytic reactor for the Photo degradation of Pharmaceutical compounds. The reactor consists of a jacketed glass tube, which houses the radiation source. A 250W UV lamp with intensity of 68.5 mW/cm² was used for the emission of visible light radiation. The mixture of drug and catalyst is taken in the outer borosilicate reactor. Cold water was circulated in the outer reactor to maintain the solution temperature. The inner glass tube is immersed in the solution of drug and Photocatalyst. The experiments were carried out for the previously optimized dosages of the Fenton's oxidation experiments.

The degradation efficiency was observed in terms of change in intensity of the drug before and after light irradiation. Photocatalytic performance was quantified by the degradation of organic pollutant under visible light irradiation.

$$\left(\frac{C_0 - C_t}{C_0}\right) \times 100 \text{ --- (1)}$$

Where, C_0 = concentration of drug solution before Photoirradiation (mg/L), C_t = Concentration of drug solution after photoirradiation (mg/L).

3.1 comparison between fenton and photo-fenton process of percent amx removal

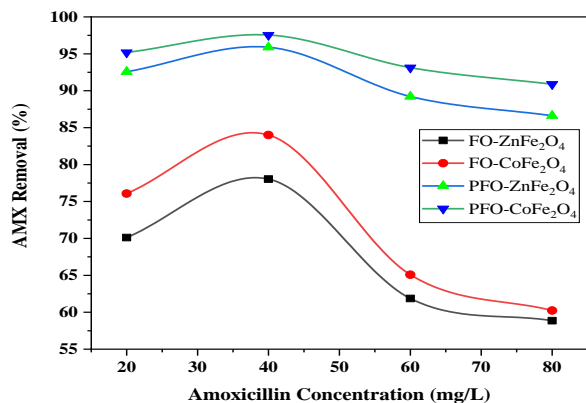


Figure 4. Comparison Between Fenton and Photo-Fenton Process of Percent AMX Removal [Reaction Conditions; [AMX]₀ = 20 to 80 mg/L, pH = 4.0, [H₂O₂] = 30 mg/L, ZnFe₂O₄ = 0.75 mg/L, CoFe₂O₄ = 0.75 mg/L, Reaction time = 120 min]

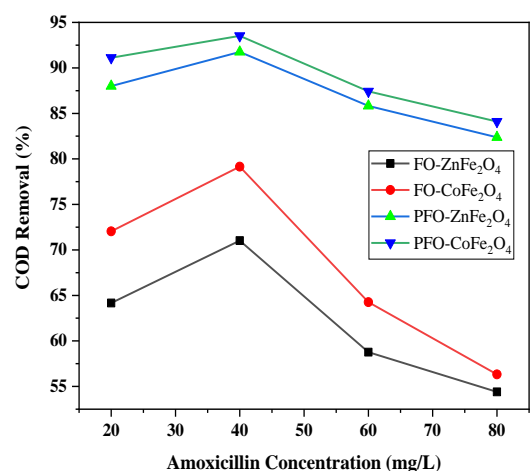


Figure 5. Comparison Between Fenton and Photo-Fenton Process of Percent COD Removal [Reaction Conditions; [AMX]₀ = 20 to 80 mg/L, pH = 4.0, [H₂O₂] = 30 mg/L, ZnFe₂O₄ = 0.75 mg/L, CoFe₂O₄ = 0.75 mg/L, Reaction time = 120 min]

The percent degradation and mineralization of AMX, is 20 to 80 mg/L initial concentration of each drug treated by Fenton oxidation and Photo-Fenton oxidation in Figure 4 to 5. The percent degradation and mineralization of AMX, is 40 mg/L of degradation of

AMX is 78.04%, with ZnFe₂O₄ in Fenton oxidation. The degradation of AMX is 84.01%, with CoFe₂O₄ in Fenton oxidation. However, during the Photo-Fenton oxidation, The degradation of AMX is 95.89%, with ZnFe₂O₄ and The degradation of AMX is 97.54% with CoFe₂O₄ in Fenton oxidation. Fenton and Photo-Fenton processes appear to effectively degrade the pharmaceutical compounds in aqueous solutions. Therefore, Fenton and Photo-Fenton oxidation using cobalt ferrite catalyst appears to be an effective and economical for the oxidation of AMX, in aqueous solution.

4. CONCLUSIONS

The XRD peaks, structural analysis of ZnFe₂O₄ and CoFe₂O₄ nanosamples, were Zinc ferrite the average particle size obtained varied between 18.63-20.45 nm based on the 2θ value, which was found to be 30.30, 35.45, 43.05, and 56.85, respectively. Similarly, for Cobalt ferrite, the average particle size obtained varied between 18.54-18.90 nm based on the 2θ value which was found to be 35.64, 40.58, 70 and 62.60 respectively. For spinel ferrites, a specific region of absorption is in the range of 400-600 cm⁻¹. Zinc Nano-ferrite exhibits two absorption bands in this region. High vibration band at 557.22 cm⁻¹ and others were at 446.5 cm⁻¹. Zinc ferrite is exhibiting an inverse spinel where Fe³⁺ ions and Zn²⁺ ions present at the tetrahedral and octahedral lattice. Cobalt nano-ferrite exhibits two absorption bands in this region. High vibration band at 570.41 cm⁻¹ and others were at 443.24 cm⁻¹. CoFe₂O₄ is exhibiting an inverse spinel where Fe³⁺ ions and Co²⁺ ions present at the tetrahedral and octahedral lattice sites respectively. SEM Image Nano Zinc ferrites show the size of the particle is around 340 nm. SEM Image Nano Cobalt ferrites show a zoomed view of the powdered sample, illustrated with both large and small grains. The nanoparticles size was found to be 308.8 nm. The degradation of AMX is 78.04%, with ZnFe₂O₄ in Fenton oxidation. The degradation of AMX is 84.01%, with CoFe₂O₄ in Fenton oxidation. However, during the Photo-Fenton oxidation, The degradation of AMX is 95.89% with ZnFe₂O₄ and The degradation of AMX is 97.54%, with CoFe₂O₄ in photo-Fenton oxidation. Mineralization of AMX is 71.02%, with ZnFe₂O₄ in Fenton oxidation. The degradation of AMX is 79.15%, with CoFe₂O₄ in

Fenton oxidation. Similarly during the Photo-Fenton oxidation, mineralization of AMX is 91.75% with ZnFe₂O₄ and The degradation of AMX is 93.52% , with CoFe₂O₄ in photo-Fenton oxidation. Therefore, Fenton and Photo-Fenton oxidation using cobalt ferrite catalyst appears to be an effective and economical for the oxidation of AMX, in aqueous solution.

REFERENCES

- [1] Sorensen, B., Nilsen, S., Lanzky, P., Ingerslev, F., Holden, H. and Jurgensen, S.E. 1998. Occurrence, fate and effect of pharmaceutical substances in the environment - A review. *J. Hazard. Mater.*, 36: 357-393.
- [2] Giger, W., Alde, A., Golet, E., Kohler, H. and Christa, S. 2003. Occurrence and fate of antibiotics as trace contaminants in wastewaters, sewage sludges and surface waters. *Chimia*, 57: 485-491.
- [3] Arslan-Alaton, I. and Dogruel, S. 2004. Pre-treatment of penicillin formulation effluent by advanced oxidation processes. *J. Hazard. Mater.*, B112: 105-113.
- [4] Otkar, H.M. and Balciolu, I.A. 2005. Adsorption and degradation of enrofloxacin, a veterinary antibiotic on natural zeolite. *J. Hazard. Mater.*, 122: 251-258.
- [5] Arikan, O.A., Rice, C. and Codling, E. 2008. Occurrence of antibiotics and hormones in a major agricultural watershed. *Desalination*, 226: 121-133.
- [6] Kummerer, K. 2003. Significance of antibiotics in the environment. *J. Antimicrob. Chemother.*, 52: 5-7.
- [7] Sponza, D.T. and Demirten, P. 2007. Treatability of sulfamerazine in sequential upflow anaerobic sludge blanket reactor (UASB)/completely stirred tank reactor (CSTR) processes. *Separ. Purif. Technol.*, 56: 108-117.
- [8] Gonzalez, O., Sans, C. and Esplugas, S. 2007. Sulfamethoxazole abatement by photo-fenton toxicity, inhibition and biodegradability assessment of intermediates. *J. Hazard. Mater.*, 146: 459-464.
- [9] Dantas, R.F., Contreras, S., Sans, C. and Esplugas, S. 2008. Sulfamethoxazole abatement by means of ozonation. *J. Hazard. Mater.*, 150: 790-794.
- [10] Li, D., Yang, M., Hub, J., Yu, Z., Chang, H. and Jin, F. 2008. Determination of penicillin G and its degradation product in penicillin production wastewater treatment plant and the receiving river. *Water Res.*, 42: 307-317.
- [11] Bautitz, I. and Nogueira, R. 2007. Degradation of tetracycline by photo-fenton process-Solar irradiation and matrix effects. *J. Photochem. Photobiol., A: Chem.* 187: 33-39.
- [12] Li, S. Z., Li, X. Y. and Wang, D.Z. 2004. Membrane (RO-UF) filtration for antibiotic wastewater treatment and recovery of antibiotics. *Separ. Purif. Technol.*, 34: 109-114.
- [13] Choi, K., Kim, S. and Kim, S.H. 2008. Removal of antibiotics by coagulation and granular activated carbon filtration. *J. Hazard. Mater.*, 151: 38-43.
- [14] Adriano, W., Veredas, V., Santana, C. and Gonçalves, L. 2005. Adsorption of amoxicillin on chitosan beads, kinetics, equilibrium and validation of finite bath models. *Biochem. Eng. J.*, 27: 132-137.
- [15] Debordea, M. and Guntena, U. 2008. Reactions of chlorine with inorganic and organic compounds during water treatment- Kinetics and mechanisms: A critical review. *Water Res.*, 42: 13-51.
- [16] Balciglu, I. and Otkar, M. 2004. Pre-treatment of antibiotic formulation wastewater by O₃, O₃/H₂O₂, and O₃ /UV Processes. *Turkish J. Eng. Env. Sci.*, 28: 325-331.
- [17] Zhang, J., Giorno, L. and Drioli, E. 2006. Study of a hybrid process combining PACs and membrane operations for antibiotic wastewater treatment. *Desalination*, 194: 101-107.
- [18] Jara C.C., Fino, D., Specchia, V., Saracco, G. and Spinelli, P. 2007. Electrochemical removal of antibiotics from wastewaters. *Appl. Catal. B: Environ.*, 70: 479-487.
- [19] Jolivet, J.P., C. Chaneac, P. Prene, L. Vayssieres, E. Tronc, 1997. Wet Chemistry of Spinel Iron oxide Particles. *J. Phys. IV France*, 7: C1-573.